Spectroscopic Studies of Structural Changes in Two β-Sheet-Forming Peptides Show an Ensemble of Structures that Unfold Noncooperatively †

ARTICLE *in* BIOCHEMISTRY · MAY 2003

Impact Factor: 3.02 · DOI: 10.1021/bi026893k · Source: PubMed

4 AUTHORS:

Serguei Kuznetsov
University of Illinois at Chicago
40 PUBLICATIONS **673** CITATIONS
SEE PROFILE

Jovencio Hilario
Bio-Rad Laboratories
12 PUBLICATIONS **444** CITATIONS
SEE PROFILE

Timothy A Keiderling
University of Illinois at Chicago
276 PUBLICATIONS **7,308** CITATIONS
SEE PROFILE

Anjum Ansari
University of Illinois at Chicago
53 PUBLICATIONS **3,093** CITATIONS
SEE PROFILE

Articles

Spectroscopic Studies of Structural Changes in Two β-Sheet-Forming Peptides Show an Ensemble of Structures that Unfold Noncooperatively†

Serguei V. Kuznetsov,‡ Jovencio Hilario,§ Timothy A. Keiderling,§ and Anjum Ansari*,‡,||

Departments of Physics (M/C 273), Chemistry (M/C 111), and Bioengineering (M/C 063), University of Illinois at Chicago, 845 West Taylor Street, Chicago, Illinois 60607

Received September 23, 2002; Revised Manuscript Received February 7, 2003

ABSTRACT: A characterization of the conformation and stability of model peptide systems that form β-sheets in aqueous solutions is considerably important in gaining insights into the mechanism of β-sheet formation in proteins. We have characterized the conformation and equilibrium folding and unfolding of two 20-residue peptides whose NMR spectra suggest a three-stranded β-sheet topology in aqueous solution: Betanova [Kortemme, T., Ramirez-Alvarado, M., and Serrano, L. (1998) *Science 281*, 253−256] and ^{D}P^{D}P with D-Pro-Gly segments at the turns [Schenck, H. L., and Gellman, S. H. (1998) *J. Am. Chem. Soc. 120*, 4869−4870]. Both circular dichroism (CD) and infrared measurements indicate only 20−26% β-sheet-like structure at 5 °C for Betanova and 42−59% β-sheet for ^{D}P^{D}P. For both peptides, the CD and infrared spectra change nearly linearly with increasing temperatures (or urea concentrations) and lack a sigmoidal signature characteristic of cooperative unfolding. Fluorescence resonance energy transfer (FRET) measurements between donor and acceptor molecules attached to the two ends confirm that Betanova is largely unstructured even at 10 °C; the average end-to-end distance estimated from FRET is closer to that of a random coil than a structured β-sheet. In ^{D}P^{D}P, the FRET results indicate a more compact structure that remains compact even at high temperatures (∼80 °C) or high urea concentrations (∼8 M). These results indicate that both these peptides access an ensemble of conformations at all temperatures or denaturant concentrations, with no significant free energy barrier separating the "folded" and "unfolded" conformations.

The elementary processes in protein folding are the hydrophobic collapse of the heteropolymer, the formation of the secondary structural elements (α-helices and β-sheets), and the rearrangement of these structural elements influenced by long-range tertiary interactions. A complete understanding of how the information for a stable and relatively unique three-dimensional protein structure is encoded in its amino acid sequence will come from a detailed investigation of each of these elementary steps. One of the exciting opportunities offered by the folding studies on small peptides is that the thermodynamics and kinetics can be compared directly with molecular dynamics simulation studies, thus providing an important benchmark for the simulation studies.

An important issue that remains unresolved from studies of model peptide systems is the degree and extent of cooperativity in the folding and unfolding at the secondary structure level without the larger context of tertiary interactions (*1*−*5*). Are the ensemble of states representative of the "folded" and "unfolded" conformations separated by a significant free energy barrier, or is there a continuum of populations? Signatures of cooperative transitions are sigmoidal changes in all order parameters that characterize the extent of thermal or denaturant-induced unfolding, and kinetics of folding and unfolding that are single-exponential. Short peptides usually exhibit very broad transitions, thus making it difficult to identify cooperativity. An important criterion for cooperative folding and unfolding is that the equilibrium transitions and/or kinetics measured with different probes of the overall conformation exhibit identical behavior.

Although the thermodynamics and kinetics of helix−coil transition have been intensively studied for several decades, there is relatively little information about the thermodynamic and kinetic factors that influence the stability of β-sheet folds. A major obstacle to the study of β-sheets has been the difficulty in isolating designed or naturally occurring β-sheet sequences that do not aggregate. In recent years, several examples of β-hairpins and β-sheets that are stable in solution, and whose thermodynamic studies reveal reversible folding−unfolding transitions, have begun to provide insights into the underlying energy landscape (*1*, *6*−*11*). These

† This work was supported, in part, by the donors of the Petroleum Research Fund administered by the American Chemical Society through Grant ACS-PRF 35443-AC4 (T.A.K.).

* To whom correspondence should be addressed. E-mail: ansari@uic.edu. Phone: (312) 996-8735. Fax: (312) 996-9016.

‡ Department of Physics.

§ Department of Chemistry.

|| Department of Bioengineering.

10.1021/bi026893k CCC: $25.00
Published on Web 03/25/2003

studies have important implications in biology, both in the design of novel protein-like molecules and in the fundamental understanding of the factors that lead to amyloid fibril formation, caused by β-sheet aggregation, which leads to many pathological diseases (*12*, *13*).

The most extensively studied model system for β-sheets is the 16-residue segment from the B1 domain of streptococcal protein G that forms a β-hairpin (*6*) and which exhibits "two-state" folding and unfolding, both in its thermodynamics (*14*) and in its kinetics (*15*, *16*). The only three-stranded β-sheet that has received much attention is a 40-residue segment called the WW domain, which also exhibits single-exponential kinetics (*17*, *18*). However, the equilibrium thermal and denaturant unfolding of WW show deviations from that expected for a simple two-state system (*17*).

In this study, we have focused on two 20-residue peptides, whose NMR spectra suggest a three-stranded β-sheet topology, to investigate further the extent of cooperativity in *de novo*-designed peptides capable of forming β-sheet structures. The first peptide, RGWSVQNGKYTNNGKTTEGR, designed by Serrano and co-workers and named Betanova, was one of the first *de novo*-designed peptides that appeared to adopt a three-stranded β-sheet in aqueous solution (*19*). Serrano and co-workers measured urea-induced unfolding of Betanova as monitored by an increase in the intensity of Trp (W3) fluorescence (*19*). In addition, they measured the thermal unfolding monitored by circular dichroism (CD)[1] ellipticity changes at 217 nm. They interpreted their results as indicating a cooperative unfolding transition. However, their fluorescence measurements were done with no control for the intrinsic changes in the quantum yield of Trp as a function of urea. Furthermore, the ellipticity changes were nearly linear with increasing temperature from ~12 to 102 °C, with only a slight hint of a "toe" in the melting profile below 12 °C. Subsequent measurements using Fourier transform infrared (FTIR) and CD spectroscopy showed that Betanova has bands that are consistent with a significant amount of random coil and perhaps some β-sheet structure, and their thermal denaturation profiles, although reversible, were not sigmoidal (*20*). Measurements using UV resonance Raman (UVRR) spectroscopy showed a disruption of the hydrophobic cluster with temperature, but no change in the peptide vibrational spectra (*21*). In a reexamination of the NMR and CD spectra of Betanova, Serrano and co-workers modified their estimate of β-sheet population from ~80%, as reported in the original study, to ~10% (*22*).

The conformation, stability, and free energy landscape of Betanova have also been investigated in molecular dynamics simulation studies (*2*, *23*). A remarkable feature of the energy landscape obtained from these studies is the lack of a free energy barrier between the compact state, with a significant fraction of "native" contacts, and the ensemble of more extended conformations. Taken together, these experimental and theoretical studies contradict the results of the original study on Betanova that described a stable three-stranded β-sheet that unfolded cooperatively (*19*). Thus, additional measurements on Betanova are warranted to gain a clearer picture of its conformation and stability.

[1] Abbreviations: FL, 5(6)-carboxyfluorescein; TMR, 5(6)-carboxytetramethylrhodamine; CD, circular dichroism; FTIR, Fourier transform infrared spectroscopy; FRET, fluorescence resonance energy transfer; UVRR, UV resonance Raman.

The second peptide in this study is VFITS^{D}PGKTYTEV^{D}PGOKILQ, which was designed by Schenck and Gellman and named ^{D}P^{D}P because of the two D-Pro-Gly segments that promote turn formation (*9*). This peptide was also reported to form a three-stranded β-sheet in aqueous solution with a CD spectrum at 24 °C that is much more characteristic of a β-sheet than the corresponding Betanova spectrum (*9*). ^{D}P^{D}P has been proposed as a model system for cooperative formation of β-sheet at the secondary structure level, without long-range tertiary interactions. Schenck and Gellman have shown that replacing one of the D-Pro-Gly segments with an L-Pro-Gly segment abolishes that hairpin and, more importantly, destabilizes the remaining hairpin; replacing both the D-Pro-Gly with L-Pro-Gly segments yields a largely random coil-like CD spectrum (*9*). However, there are no measurements on the thermodynamics of unfolding of ^{D}P^{D}P. A comparison of the thermodynamics of ^{D}P^{D}P, which has well-defined nucleation sites at the turns, with model systems such as Betanova without turn nucleation should reveal further insights into the relative importance of the factors that initiate and stabilize β-sheet formation.

In this paper, we report a detailed thermodynamic investigation of these two peptides of similar lengths but which exhibit very different β-sheet conformations as indicated by their low-temperature CD and FTIR spectra, with the view of comparing their conformations and unfolding behavior. In addition to the standard spectroscopic probes such as CD, FTIR, and intrinsic fluorescence, we report the first estimate of the end-to-end distance of these peptides using fluorescence resonance energy transfer (FRET) measurements between extrinsic donor and acceptor dyes attached to the C- and N-termini. FRET measurements provide a sensitive probe of changes in intermolecular distances and hence the overall compactness of the polypeptide as a function of temperature and denaturant concentrations (*24*−*26*). These measurements provide a basis for future studies aimed at understanding the kinetics and thermodynamics of three-stranded β-sheet folding.

MATERIALS AND METHODS

Materials and Sample Preparation. All peptides without extrinsic fluorescence labels were synthesized at the Protein Research Facility at the University of Illinois at Chicago. Peptides labeled for FRET measurements were purchased from Biopeptide Co. (San Diego, CA) and were synthesized with Lys at the C-terminus. For both Betanova and ^{D}P^{D}P, the donor was 5(6)-carboxyfluorescein (FL), attached to Lys at the C-terminus, and the acceptor was 5(6)-carboxytetramethylrhodamine (TMR), attached to the N-terminus. All samples were HPLC purified, and the accuracy of the labeling was determined by mass spectroscopy. For CD reference spectra, we used a cyclic peptide, cyclo-(RYVEV^{D}PGOKILQ^{D}PG), with the first and last residues covalently linked via a peptide bond. This peptide was a generous gift of S. H. Gellman from the University of Wisconsin (Madison, WI) and poly(L-lysine), which was obtained from Sigma (St. Louis, MO). Fluorescein (F-1300, Molecular Probes, Eugene, OR) was used for standard measurements of fluorescence quantum yield.

Thermal Denaturation Measurements Using CD and FTIR. Static CD measurements in the range of 190−250 nm were

taken with a JASCO (Easton, MD) J-600 spectropolarimeter. The peptide concentration was 0.2 mg/mL (~89 μM) for Betanova in 1 mM sodium cacodylate buffer at pH 4.8 and 0.2 mg/mL (~85 μM) for $^{D}P^{D}P$ in 100 mM acetate/D_2O, pH 3.8 buffer. The CD measurements were made in a cell with a path length of 0.5 mm. The sample temperature was controlled with a circulating water bath (model 9100, Fisher Scientific) and measured with a digital thermometer (model HH503, Omega, Stamford, CT) equipped with a type K thermocouple, which was placed directly inside the sample cell. Samples were allowed to equilibrate at each temperature for ~5 min. CD measurements were taken approximately every 5 °C in the temperature range of 5−95 °C. Typically, eight scans were collected at each temperature at a scanning speed of 20 nm/min with a 2.0 nm bandwidth and a 2 s response time. All spectra were corrected by subtracting the spectra of the appropriate buffers.

FTIR measurements of the amide I′ (N−D-exchanged C═O stretch) were taken with a Digilab (Randolph, MA) FTS-60A spectrometer. The peptide concentrations were 20 mg/mL (~8.9 mM for Betanova and ~8.5 mM for $^{D}P^{D}P$). Excess trifluoroacetic acid (TFA) remaining from the peptide synthesis, and whose IR absorption at 1672 cm^{-1} can interfere with amide I′ vibrations, was removed by dissolving the peptide in dilute HCl (~10 mM) and then lyophilized to a powder. Powdered samples were dissolved in approximately 30 μL of buffer (100 mM sodium cacodylate buffer at pH 4.8 for Betanova and 100 mM acetate/D_2O, pH 3.8 buffer for $^{D}P^{D}P$) and placed between two CaF_2 windows separated by a 50 μm spacer. The windows were held together in a brass compression ring and placed in a water-jacketed holder attached to a circulating water bath (model RTE-110, Neslab). To allow for exchange of amide protons with deuterium, samples were heated in their cells at 40 °C for ~2 h and then cooled rapidly to 4 °C. Spectra were measured in the temperature range of 4−92 °C. Approximately 300 symmetric interferograms were collected at 4 cm^{-1} resolution at each temperature.

Thermal and Urea Denaturation Measurements Using Trp and Tyr Fluorescence. Static measurements of the intrinsic fluorescence of Betanova, with excitation at 295 and 274 nm, were obtained as a function of temperature and urea concentration. The fluorescence emission spectra were measured using a FluoroMax-2 spectrofluorometer (Jobin Yvon-Spex, Edison, NJ). The sample temperature was controlled by a circulating water bath (model RTE-110, Neslab) and measured using a YSI 44008 thermistor (YSI, Inc., Yellow Springs, OH) in direct contact with the sample cell. The peptide concentration was ~100 μM for thermal unfolding measurements with excitation at 295 nm, ~119 μM for thermal unfolding measurements with excitation at 274 nm, and ~119 μM for urea unfolding measurements. The solvent used for all measurements was 5 mM sodium acetate buffer (pH 5) which was chosen so the solvent would be identical to that used by Serrano and co-workers (*19*).

For each set of fluorescence measurements on Betanova, a corresponding set of measurements was made on reference peptides that were five residues long, under solvent conditions identical to those for the Betanova measurements. The five-residue reference peptides were fragments from the Betanova sequence: RGWSV and GKYTN for Trp and Tyr measurements, respectively. The concentrations of the reference peptides relative to that of Betanova were determined accurately by a least-squares fit of the absorption spectrum of Betanova in the range of 240−330 nm with linear combinations of the absorption spectra of the reference peptides.

Deconvolution of Trp and Tyr Components in Betanova. Two sets of fluorescence measurements were taken with Betanova: one with excitation at 295 nm, to excite Trp fluorescence only, and the other at 274 nm, which also excites Tyr fluorescence. Excitation at 274 nm leads to fluorescence emission from both W3 and Y10 in Betanova, with the component from Y10 as only a small shoulder on the much larger W3 fluorescence. To determine the relative contributions of W3 and Y10 to the measured spectra of Betanova under each set of conditions, we used the following approach. First, the fluorescence of reference peptides RGWSV and GKYTN were measured under identical conditions and normalized to the same concentration as Betanova. Next, the contribution of W3 in Betanova was determined by fitting the spectra of RGWSV to the Betanova spectra in the wavelength range of 345−450 nm, where there is no contribution from Y10. The emission spectra of RGWSV were shifted to the blue by ~2.5 nm to account for the small spectral shifts in Trp fluorescence between Betanova and RGWSV. Next, the W3 contribution was subtracted from Betanova to obtain the Y10 component as a function of condition, and which could be directly compared with the corresponding amplitude of Tyr fluorescence in the reference peptide GKYTN, for each set of conditions.

FRET Measurements. Three sets of FRET measurements were taken: (i) thermal unfolding of Betanova, (ii) thermal unfolding of $^{D}P^{D}P$, and (iii) urea unfolding of $^{D}P^{D}P$. The sample concentrations for all FRET measurements were ~10 μM. For Betanova, the solvent was 5 mM sodium acetate buffer (pH 5), and for $^{D}P^{D}P$, the solvent was 100 mM sodium acetate buffer (pH 3.8). For each set of measurements, the fluorescence emission spectra were measured in the wavelength range of 460−750 nm, for the peptides with only the donor attached (peptide-FL) and for the peptides with both the donor and acceptor attached at either end (TMR-peptide-FL), after excitation at 450 nm where there is negligible absorption from TMR. The efficiency of energy transfer from the donor to the acceptor was determined from the equation $E = 1 - (I_{DA}/I_D)$, where I_{DA} and I_D are the fluorescence intensities of the donor with and without the acceptor, respectively. The I_{DA}/I_D ratio was obtained from a least-squares fit of the blue edge of the fluorescence emission spectra of peptide-FL to the blue edge of TMR-peptide-FL, in the wavelength range of 460−540 nm, where there is no contribution from the TMR fluorescence. The multiplicative factor required to scale the peptide-FL fluorescence to the TMR-peptide-FL fluorescence, after correcting for the differences in the concentrations of the two samples, gives directly the I_{DA}/I_D ratio, and hence the efficiency of energy transfer E, under each set of conditions.

Determination of the Forster Distance R_o. The efficiency of energy transfer is related to the distance between the two probe molecules, R, by the equation $E = 1/[1 + (R/R_o)^6]$, where R_o is the Forster distance at which the efficiency of energy transfer is 50%. The Forster distance (in angstroms)

Table 1: Measurements for Calculation of Forster Distances[a]

sample	ϕ_d[b]	J[b] (M^{-1} cm^{-1} nm^4)	n[c]	R_o[b] (Å)	R (Å)
Betanova (25 °C)	0.30	2.68×10^{15}	1.33	46	45
Betanova (80 °C)	0.25	2.68×10^{15}	1.32	44	46
^{D}P^{D}P (25 °C)	0.27	2.97×10^{15}	1.33	45	31
^{D}P^{D}P (80 °C)	0.17	2.97×10^{15}	1.32	43	31
^{D}P^{D}P (8 M urea at 25 °C)	0.22	3.75×10^{15}	1.40	45	31

[a] The notations are as described in Materials and Methods. [b] The standard errors are estimated to be ±0.02 for ϕ_d, $\pm 0.15 \times 10^{15}$ M^{-1} cm^{-1} nm^4 for J, and ±1 Å for R_o. [c] The values of the refractive indices are from the *CRC Handbook of Chemistry and Physics*, 63rd ed., CRC Press, Boca Raton, FL.

was calculated from $R_o = (9.79 \times 10^3)(\kappa^2 n^{-4} \phi_d J)^{1/6}$, where κ^2 is the orientation factor, n is the refractive index of the solvent, ϕ_d is the quantum yield of the donor in the absence of the acceptor, and J is the spectral overlap integral [$J = \int_0^\infty F_d(\lambda)\epsilon_a(\lambda)\lambda^4\, d\lambda$]. Here $F_d(\lambda)$ is the normalized fluorescence intensity of the donor (normalized to unit integrated intensity) and $\epsilon_a(\lambda)$ is the molar extinction coefficient of the acceptor (*27*). ϕ_d and $F_d(\lambda)$ were determined for both peptides by measuring the fluorescence emission spectra of peptide-FL at all temperatures and urea concentrations used in the FRET measurements. The emission spectrum of fluorescein at pH 13, with a quantum yield of 0.92, was used as a standard reference (*28*). $\epsilon_a(\lambda)$ was obtained from the absorbance spectrum of TMR-peptide-FL at two reference temperatures, 25 and 80 °C, for both peptides, and additionally at two reference urea concentrations, 0 and 8 M, for TMR-^{D}P^{D}P-FL, at 25 °C. The measured absorbance spectrum of the doubly labeled peptide was fitted to a linear combination of the spectral profile of peptide-FL, measured under the same condition, and the spectral profile of free TMR. The contribution of the FL component was then subtracted to obtain the absorption spectrum of the TMR component, and the molar extinction values were determined from the measured concentrations of the TMR-peptide-FL samples. The overlap integrals were determined by numerical integration of the normalized emission spectrum of peptide-FL and the $\epsilon_a(\lambda)$ of the TMR component in TMR-peptide-FL. The results of these measurements and the corresponding R_o values (assuming a κ^2 value of $^2/_3$) are summarized in Table 1 in the Results.

Singular-Value Decomposition Analysis. The raw data in the fluorescence, CD, or FTIR measurements, consisting of spectra as a function of condition (temperature or urea concentration), were first filtered using singular-value decomposition (SVD) prior to any further analysis. SVD transforms the data matrix **D** into a product of three matrices, i.e., $\mathbf{D} = \mathbf{USV^T}$ (*29*). The columns of **U** are a set of orthonormal basis spectra that describe all the spectra in the data matrix **D**; the columns of **V** are the corresponding amplitudes as a function of condition, and **S** is a diagonal matrix with non-negative elements called the singular values which are a measure of the contribution of the corresponding basis spectrum to the data matrix. SVD has the useful property of the components with the k largest singular values providing the best (in the least-squares sense) k-component fit to the data. The spectra that were used for further analysis were reconstructed from the first three basis spectra.

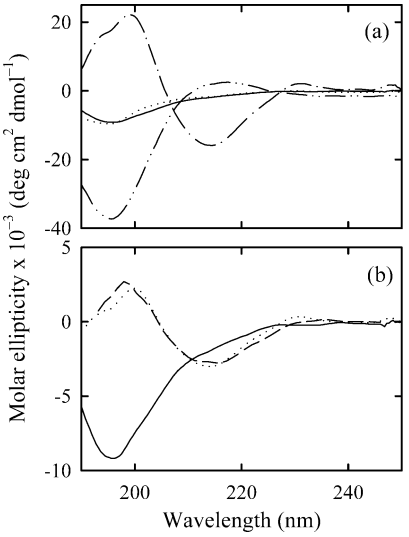

FIGURE 1: Far-UV CD spectra of Betanova and ^{D}P^{D}P. (a) The CD spectrum of Betanova at 5 °C (—) is compared with a characteristic random coil spectrum (—••—) and a characteristic β-sheet spectrum (—•—). A linear combination of the two reference spectra that best fits the Betanova spectrum at 5 °C (•••) yields ~22% β-sheet and ~78% random coil. (b) The CD spectrum of ^{D}P^{D}P at 8 °C (— — —) is compared with that of Betanova at 5 °C (—). A linear combination of the two reference spectra shown in panel a that best describes the ^{D}P^{D}P spectrum at 8 °C (•••) yields ~53% β-sheet and ~47% random coil.

RESULTS

Far-UV CD Spectra of Betanova and $^{D}P^{D}P$. The far-UV CD spectrum of Betanova at 5 °C is shown in Figure 1a. The CD spectrum of poly(L-lysine), which adopts a random coil structure in D_2O at pH 7 (*30*), is shown for comparison. We also measured the CD spectrum of cyclo-(RYVEV^{D}-PGOKILQ^{D}PG), which exhibits a very high population of antiparallel β-sheet conformation as shown by NMR data (*31*). This peptide exhibits a typical β-sheet spectrum, very similar to the standard β-sheet spectrum seen in poly(L-lysine) at pH 11 and 51 °C, with a minimum at 217 nm and a zero crossing at 205 nm (*30*, *32*). As reported previously, the CD spectrum of Betanova in the far-UV region is not very β-sheet-like (*20*). It is apparent that the Betanova band shape more closely resembles that of the random coil than a β-sheet. In the simplest analysis to determine the extent of β-sheet content in Betanova, we expressed its CD spectral shape as a linear combination of the reference random coil and β-sheet spectra. We assumed that the CD spectrum of the reference cyclic peptide has a β-sheet contribution of ~71%; i.e., 10 of the 14 residues form the β-sheet, with the remaining residues forming the two turns. The coefficients that describe the contribution of the reference spectra to the measured peptide spectra were normalized to 100%. This analysis yields ~22% β-sheet and ~78% random coil for Betanova at 5 °C (Figure 1a).

It is important to note that the molar ellipticity of Betanova is much weaker than the molar ellipticity of our model peptides. Also, the aromatic side chains can distort the CD spectral profile from that of a typical β-sheet (*33*), which has not been taken into account in our analysis. As an alternative estimate of β-sheet content, we used the factor analysis/restricted multiple-regression algorithm of Pancoska et al. (*34*) referenced to the CD spectra of 23 proteins whose

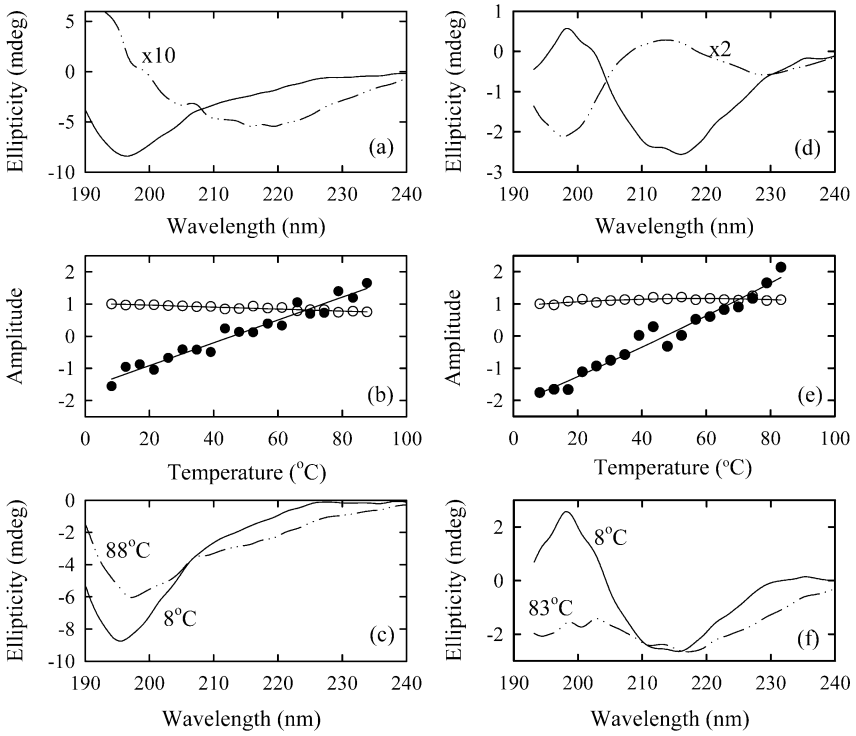

FIGURE 2: Temperature dependence of the far-UV CD spectra. The first two basis spectra of Betanova (a) and $^{D}P^{D}P$ (d) were obtained from an SVD analysis of the measured spectra as a function of wavelength. The first basis spectrum (—) represents the average shape of the spectrum, averaged over all temperatures; the second basis spectrum (—··—) represents the deviations in the shape of the spectrum. The basis spectra have been multiplied by the corresponding singular values and by the amplitude of the first component at the lowest temperature so that the spectra are in units of ellipticity. The second basis spectrum has been amplified by a factor of 10 for Betanova (a) and by a factor of 2 for $^{D}P^{D}P$ (d). The amplitudes of the first (○) and second (●) basis spectra of Betanova (b) and $^{D}P^{D}P$ (e) as a function of temperature are shown. The amplitudes are normalized such that the amplitude of the first component at the lowest temperature is equal to 1. The lines are drawn to guide the eye. The CD spectra of Betanova (c) and $^{D}P^{D}P$ (f) at the lowest and highest temperatures in our measurements are shown.

structures are well-known from X-ray crystallography. This analysis yields ~26% β-sheet content in Betanova at 5 °C.

In Figure 1b, we compare the CD spectrum of $^{D}P^{D}P$ at 8 °C with that of Betanova. The spectral shape of $^{D}P^{D}P$ is obviously much closer to that of a typical β-sheet, although its molar ellipticity is also much weaker than that of the model peptides. Partitioning of this $^{D}P^{D}P$ spectrum into the two reference CD spectra gives ~53% β-sheet structure and ~47% random coil. We also estimated the β-sheet content of $^{D}P^{D}P$ using the factor analysis algorithm and obtained ~44% β-sheet.

Thermal Denaturation of Betanova and $^{D}P^{D}P$ Monitored with Far-UV CD. The changes in the secondary structure of Betanova and $^{D}P^{D}P$ were monitored as a function of increasing temperature by measuring the far-UV CD spectra. The data, consisting of spectra as a function of temperature, were first filtered using the singular-value decomposition (SVD) procedure, as described in Materials and Methods. The first basis spectrum represents the average shape of all the temperature-dependent CD spectra in the data matrix, and the second basis spectrum represents the largest deviations from the average shape. The corresponding amplitudes monitor the temperature dependence of the contribution of each basis spectrum to the measured spectra. Higher-order components contributed less than 3% to the measured spectra.

The first two basis spectra and their corresponding amplitudes for Betanova are plotted in panels a and b of Figure 2. Both spectral components obtained from the SVD analysis exhibit nearly linear changes with increasing temperatures (Figure 2b). In Figure 2c, we compare the CD spectra at 8 and 88 °C. The negative ellipticity at ~195 nm diminishes in amplitude from approximately −9 mdeg to approximately −6 mdeg as the temperature is increased, indicating an increased level of disorder in the structure with increasing temperature. A corresponding increase in the magnitude of the (negative) ellipticity in the range of 220−240 nm is observed.

For $^{D}P^{D}P$, the changes in the CD spectrum as a function of temperature are much larger, compared to those in Betanova, as indicated by the magnitude of the second component of the SVD analysis (Figure 2d). The spectral changes in $^{D}P^{D}P$ also do not exhibit any noticeable cooperativity with increasing temperature (Figure 2e). At high temperatures, the positive peak at ~195 nm disappears, suggesting that the β-sheet secondary structure is essentially lost at ~80 °C but the local turns may have some residual population, as suggested by the non-zero CD between 210 and 230 nm (Figure 2f).

Thermal Denaturation of Betanova and $^{D}P^{D}P$ Monitored with FTIR. As an independent probe of the secondary structure content, we measured FTIR spectra of Betanova and $^{D}P^{D}P$ as a function of temperature (Figure 3). These spectra monitor the amide I′ absorption band, arising primarily from the amide C═O stretching vibrations. The SVD analysis of the temperature dependence of the FTIR spectra of Betanova is summarized in Figure 3a−c. The primary changes in the FTIR spectra are a decrease in the average amplitude with increasing temperature and a shift

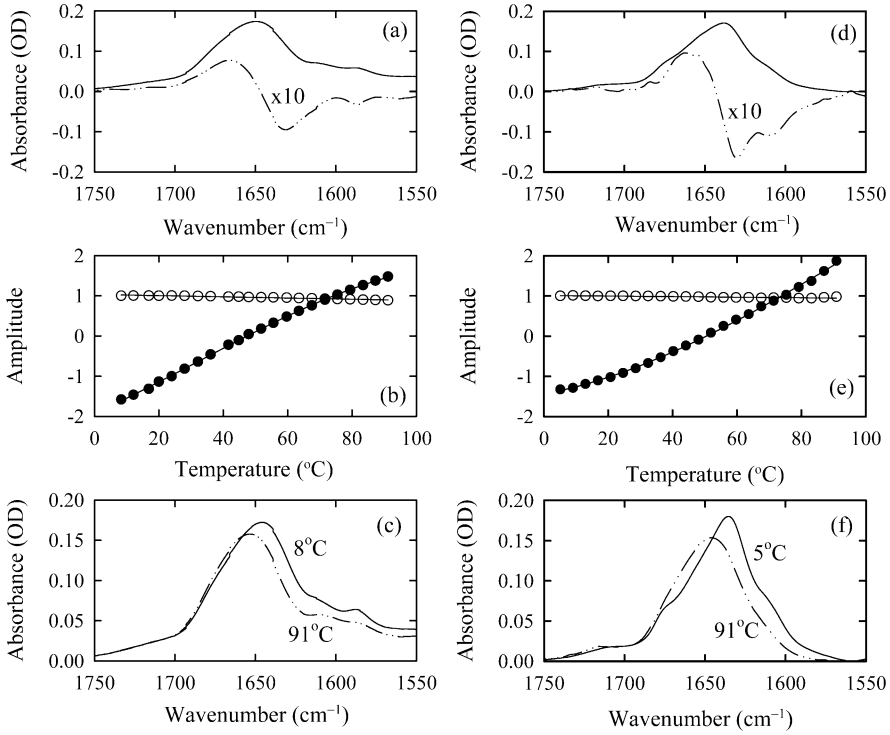

FIGURE 3: Temperature dependence of the FTIR spectra. The first two basis spectra of Betanova (a) and $^{D}P^{D}P$ (d) were obtained from an SVD analysis of the measured spectra as a function of wavelength: first component (—) and second component (—••—). The second basis spectrum has been amplified by a factor of 10 for both Betanova and $^{D}P^{D}P$. The amplitudes of the first (○) and second (●) basis spectra of Betanova (b) and $^{D}P^{D}P$ (e) as a function of temperature are shown. The lines are drawn to guide the eye. The spectra and their amplitudes are normalized as described in the legend of Figure 2. The FTIR spectra of Betanova (c) and $^{D}P^{D}P$ (f) at the lowest and highest temperatures in our measurements are shown.

of the spectrum to higher wavenumbers. Again, the amplitudes of both SVD components change nearly linearly with temperature (Figure 3b). The SVD analysis of the temperature dependence of the FTIR spectra of $^{D}P^{D}P$ is summarized in Figure 3d−f. As in Betanova, the temperature-dependent changes in the FTIR spectra of $^{D}P^{D}P$ are nearly linear but do show a slight toe at low temperatures, suggesting an approach to a stable low-temperature structure.

The FTIR spectra can also be used to estimate secondary structure content in a number of ways. In one approach, we analyzed the FTIR spectra by Fourier self-deconvolution of the amide I′ band and fitted the components to a sum of Gaussian bands, each of which corresponded to extrema in the second derivative of the amide I′ FTIR absorbance (*35*). The relative areas of bands assigned to β-sheet and random coil predict β-sheet contents of 20 and 59% for Betanova and $^{D}P^{D}P$, respectively. As a check, in the $^{D}P^{D}P$ case, the Xxx-Pro amide has a unique amide I′ band at ∼1609 cm^{-1} and contributes ∼11% to the area, which is in excellent agreement with the expected contribution of two out of 20 peptides. Alternatively, we used band shape methods based on the same factor analysis/restricted multiple-regression approach used above for CD data with our basis set of 17 protein FTIR spectra (*34*, *36*), and predicted 26 and 42% β-sheet content for Betanova and $^{D}P^{D}P$, respectively. The β-sheet contents obtained from the FTIR analysis for both peptides are in good agreement with the CD results.

Thermal and Urea Denaturation of Betanova Monitored with Intrinsic Fluorescence. We monitored the unfolding of Betanova using two sets of measurements with intrinsic fluorescent probes. In the first set of measurements, we monitored the fluorescence of W3 from 300 to 450 nm, after excitation at 295 nm. As a control, we also monitored the fluorescence of a five-residue fragment of Betanova, RGWSV, under the same set of conditions. The local environment of Trp in the peptide fragment mimics closely the environment of W3 in Betanova, making it a more appropriate choice for reference spectra than free Trp. The temperature and urea dependencies of the fluorescence intensity of RGWSV, after correcting for differences in concentration between the reference peptide and Betanova, were found to be identical to that of W3 in Betanova in the ranges of 10−80 °C (Figure 4a) and 0−9.75 M urea (Figure 4b). Our primary conclusion from these measurements is that W3 fluorescence is not a very sensitive probe of the conformational state of Betanova; the temperature and urea dependencies of W3 are dominated by the intrinsic changes in the quantum yield, and the behavior is identical, to within our signal-to-noise ratio, to the temperature and urea dependencies of the reference peptide. These results are in contradiction with the conclusions drawn by Kortemme et al. (*19*), who suggested that Betanova unfolds cooperatively with increasing urea concentration, based on their measurements of changes in W3 fluorescence.

In the second set of measurements, we measured the fluorescence emission spectra from 285 to 450 nm, with excitation at 274 nm, which maximizes the excitation of Tyr. According to the NMR data of Kortemme et al. (*19*), as well as the molecular dynamics simulations of Bursulaya and Brooks (*2*), Y10 is part of a hydrophobic cluster, together with W3, Val (V5), Asn (N12), and Thr (T17), which stabilizes the three-stranded β-sheet conformation. Tyr and Trp also form a donor−acceptor pair for fluorescence resonance energy transfer (*27*). Therefore, disruption of the

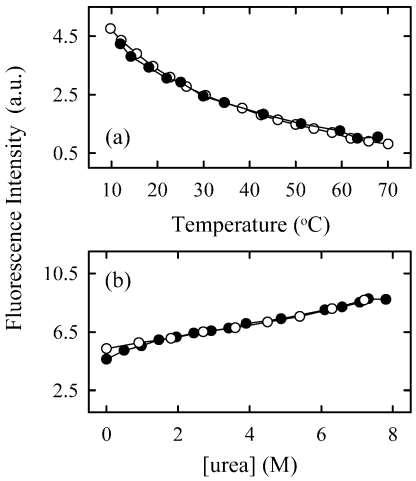

FIGURE 4: Comparison of the fluorescence properties of Trp in Betanova (W3) and in the reference peptide RGWSV, with excitation at 295 nm. (a) Amplitudes of the fluorescence emission spectra of W3 (●) and RGWSV (○) vs temperature. (b) Amplitudes of the fluorescence emission spectra of W3 (●) and RGWSV (○) as a function of urea concentration. The amplitudes of RGWSV have been corrected only for the differences in concentration between the RGWSV and Betanova samples.

hydrophobic cluster should result in an increase in the average distance between Y10 and W3, and hence a relative increase in the fluorescence of Y10. The fluorescence emission spectra, with excitation at 274 nm, show two components; the dominant one is from the W3 fluorescence, which is also excited at 274 nm, and a shoulder at the blue edge is from the Y10 fluorescence (Figure 5a,c). For reference spectra, we monitored the fluorescence of RGWSV and another five-residue fragment of Betanova, GKYTN, with excitation at 274 nm (Figure 5b). The fluorescence intensities of the W3 component in Betanova are marginally larger than the corresponding intensities in RGWSV. The fluorescence intensities of the Y10 component in Betanova are smaller by about a factor of 2 than the corresponding intensities in GKYTN. This drop in the fluorescence of Y10 relative to GKYTN and the slight increase in W3 relative to RGWSV may be attributed, in part, to resonance energy transfer from Y10 to W3 in Betanova (*27*).

The dominant effect of temperature on the fluorescence of W3 and Y10, and the reference peptides, is a decrease in the quantum yield with increasing temperature. However, as the temperature increases and Betanova unfolds, the distance between Y10 and W3 is expected to increase, thus decreasing the efficiency of energy transfer and increasing the intensity of Y10 relative to that of the reference peptide GKYTN. We can see this effect by plotting the ratio of the Y10 component in Betanova and GKYTN as a function of temperature (Figure 5d). The change in this ratio is the only signature of cooperativity we find in Betanova, which suggests that perhaps there is some cooperativity in the thermal disruption of the hydrophobic cluster. Figure 6 shows the increase in Y10 fluorescence, relative to the reference peptide GKYTN, with increasing temperature for two different concentrations of urea (0 and 4.5 M), as well as with increasing urea concentrations (Figure 6, inset). These independent sets of measurements provide a consistency check for the calculated ratio, with reproducible values obtained under identical temperature and urea conditions. The primary source of noise in these measurements is the difficulty in estimating the amplitude of the small Tyr component in Betanova relative to the large amplitude of the Trp component, especially at low temperatures (Figure 5a,c). These results indicate that the hydrophobic cluster is disrupted as the temperature is increased or the urea concentration increased, with some evidence, albeit weak, that this disruption is cooperative.

Thermal and Urea Denaturation of Betanova and $^{D}P^{D}P$ Using FRET Measurements with Extrinsic Labels. The strongest support for a β-sheet topology of Betanova under

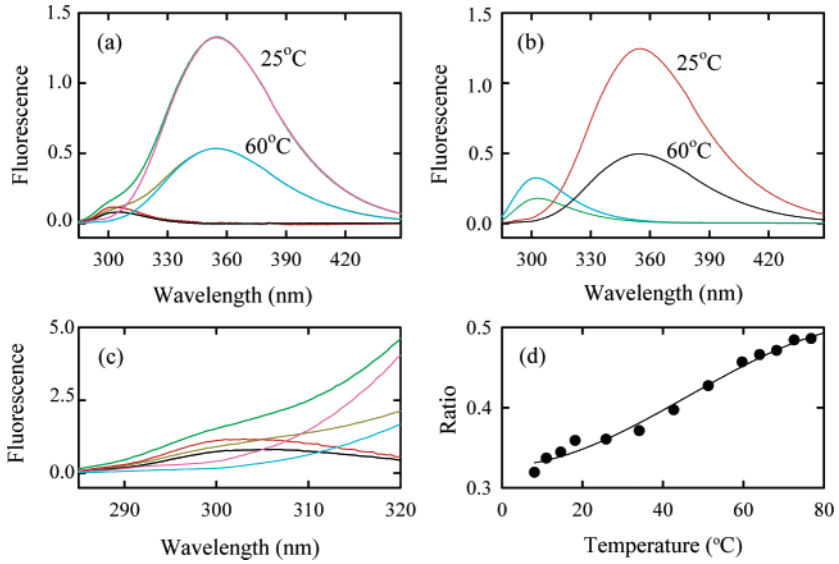

FIGURE 5: Fluorescence emission spectra of Betanova with excitation at 274 nm. (a) The fluorescence spectra of Betanova at 25 °C (green) and 60 °C (brown) are shown; the deconvoluted components at 25 °C are Tyr (red) and Trp (pink) and at 60 °C are Tyr (black) and Trp (blue). The Tyr and Trp components are centered at ~300 and ~355 nm, respectively. (b) Tyr emission spectrum in the reference peptide GKYTN at 25 °C (blue) and 60 °C (green) and Trp emission spectrum in the RGWSV reference peptide at 25 °C (red) and 60 °C (black). In all cases, excitation is at 274 nm. The concentrations of the reference peptides have been normalized to match the concentration of Betanova. (c) The lower left corner of panel a is amplified to show the Tyr components more clearly. (d) The ratio of the amplitudes of the Tyr component in Betanova and that in the reference peptide GKYTN is plotted vs temperature. The line is drawn to guide the eye.

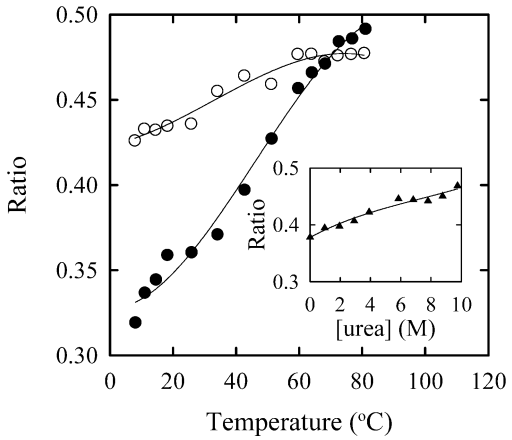

FIGURE 6: Temperature and urea dependence of the Tyr component in Betanova. The ratio of the Tyr component in Betanova and that in the GKYTN reference peptide is plotted vs temperature: (●) identical to the data in Figure 5d and (○) in 4.5 M urea. The inset shows the corresponding ratio as a function of urea concentration at 25 °C. The lines are drawn to guide the eye.

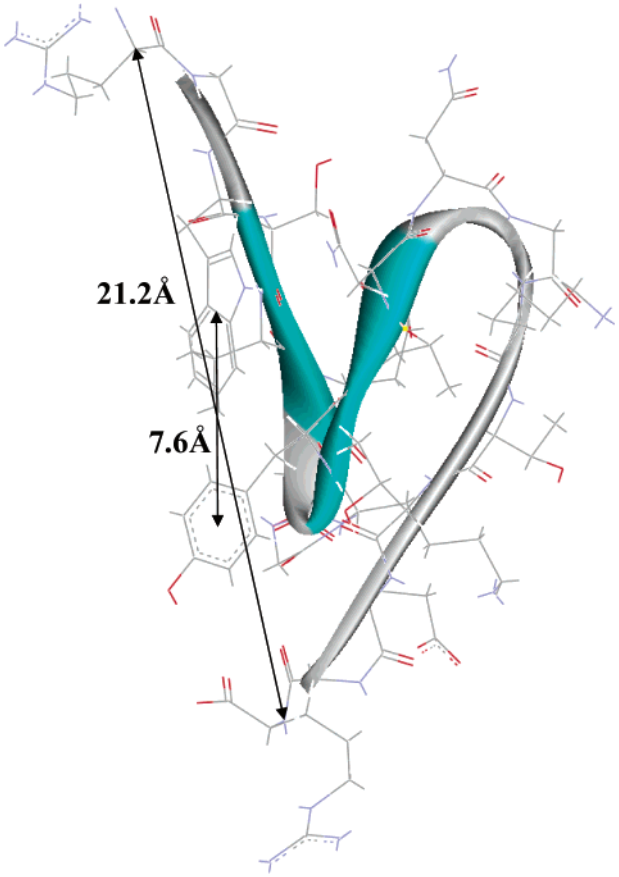

FIGURE 7: Minimized average NMR structure of Betanova at 0−7 °C (*19*).

native conditions came from the original NMR data of Serrano and co-workers (*19*); their data indicate a distance of ∼21 Å between the C_α atoms of the N- and C-termini for the folded conformation (Figure 7). Here we have taken FRET measurements between fluorescent labels attached to the ends of the peptide to estimate the distance between the two ends.

We measured the fluorescence emission spectra of Betanova labeled with only fluorescein (FL) at the C-terminus (Betanova-FL) and with both tetramethylrhodamine (TMR)

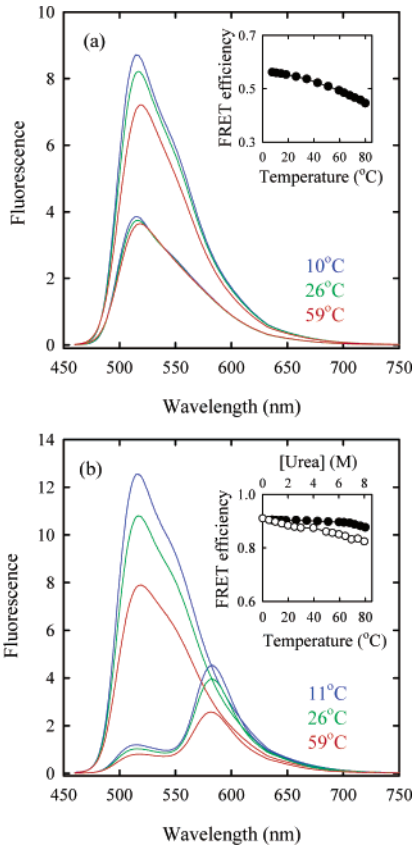

FIGURE 8: Equilibrium FRET measurements on Betanova and $^{D}P^{D}P$. The fluorescence emission spectra of (a) Betanova-FL (top three curves) and TMR-Betanova-FL (bottom three curves) and (b) $^{D}P^{D}P$-FL (top three curves) and TMR-$^{D}P^{D}P$-FL (bottom three curves), after excitation at 450 nm, are plotted at three different temperatures. The inset shows the ratio of the amplitudes of the fluorescein component in TMR-peptide-FL (I_{DA}) and that in peptide-FL (I_D) plotted vs temperature (●) and urea concentration (○).

and FL at the N- and C-termini, respectively (TMR-Betanova-FL), with excitation at 450 nm. The fluorescence intensity of FL in TMR-Betanova-FL is smaller by a factor of ∼2 than the corresponding intensity in Betanova-FL, measured under identical conditions (Figure 8a). This drop in intensity arises from resonance energy transfer from FL (the donor) to TMR (the acceptor). To obtain the efficiency of energy transfer between the donor and the acceptor, we calculated the I_{DA}/I_D ratio from the FRET measurements, where I_{DA} and I_D are the fluorescence intensity of the donor with and without the acceptor, respectively (see Materials and Methods). The primary conclusion that can be drawn from these measurements is that the efficiency of energy transfer changes very little as a function of temperature (inset of Figure 8a), from ∼56% at 10 °C to ∼44% at 80 °C, indicating that the average end-to-end distance of this peptide remains close to the Forster distance R_o at all temperatures.

The values of R_o, calculated using the measured values of the quantum yield of the donor and the overlap integral at two reference points for each set of FRET measurements, are summarized in Table 1, together with the estimated values of the average end-to-end distance between the two fluorescent probes. The observed changes in FRET efficiency arise primarily from changes in the quantum yield of the donor and hence R_o (see Table 1). The most notable conclusion here is that, for Betanova, the average distance

between the two fluorescent probes, even at the lowest temperature in our measurements, is found to be ~45 Å, with practically no change observed under thermal denaturation. To model this distance, we took the β-sheet conformation obtained from the NMR analysis of Kortemme et al. (*19*) for Betanova shown in Figure 7, and estimated the distance between FL, attached through an additional Lys at the C-terminus, and TMR attached to the N-terminus. Allowing full rotation of the amide link to each fluorescent probe, the center-to-center distance between the probes is estimated to be in the range of 29−34 Å, which is considerably smaller than the distance estimated from FRET measurements. These results support our conclusion from the CD and FTIR analysis that the β-sheet population in Betanova is very small and that the thermal denaturation change is modest.

For comparison, we also made FRET measurements on ^{D}P^{D}P, which exhibits a more complete β-sheet conformation than Betanova, as suggested by its low-temperature CD and FTIR spectra and NMR data at 24 °C (*9*). The fluorescence emission spectra of ^{D}P^{D}P labeled with the donor only, ^{D}P^{D}P-FL, and labeled with the donor and acceptor, TMR-^{D}P^{D}P-FL, were recorded as a function of temperature after excitation at 450 nm. The emission spectra of TMR-^{D}P^{D}P-FL now clearly show two components: one from the fluorescence of FL and another one from TMR (Figure 8b).[2] The intensity of the FL component in the doubly labeled peptide is now almost a factor of 10 smaller than the corresponding intensity in the singly labeled peptide, indicating ~90% FRET efficiency in this peptide. With increasing temperatures, the FRET efficiency varies from ~91% at 7 °C to ~88% at 80 °C; with increasing urea concentrations, the FRET efficiency varies from ~91% (at 0 M urea) to ~82% (at 8 M urea) (inset of Figure 8b). The average end-to-end distance for this peptide is estimated to be ~31 Å at 25 °C, again with essentially no change in the distance with increasing temperatures or increasing urea concentrations (see Table 1). For the folded topology of ^{D}P^{D}P, based on model building using typical three-stranded β-sheet conformational parameters and the design conformation of the D-Pro-Gly turns, we estimate the center-to-center distance between the two fluorescent probes, TMR on the N-terminus and FL attached to the side chain of a Lys added to the C-terminus, to be in the range of 30−35 Å. This estimate is in excellent agreement with the end-to-end distance estimated from FRET measurements on ^{D}P^{D}P. The FRET results, therefore, clearly demonstrate that in the structured ^{D}P^{D}P the ends are much closer than in the apparently less structured Betanova.

One concern when attaching fluorescent labels to peptides is that the labeling may disturb the conformations of the peptides. As a check of how much the labels perturb the structure, we compared the CD spectra of Betanova and ^{D}P^{D}P at 5 °C, in the range of 190−260 nm, with and without fluorescent labels. The CD spectra of the labeled peptides were found to be identical, within experimental error, to that of the unlabeled peptides, indicating that neither the labels nor the Lys at the C-terminus significantly perturbs the structure.

DISCUSSION

The major focus of this study is a thorough thermodynamic investigation of two short peptides, Betanova and ^{D}P^{D}P, designed to adopt three-stranded β-sheet structures. We find that, for both peptides, the CD and FTIR spectra change nearly linearly with temperature. Our measurements of the changes in the CD ellipticity of Betanova at 217 nm with increasing temperatures are in agreement with the measurements of Kortemme et al.; however we cannot conclude from our CD measurements that the thermal unfolding of Betanova is cooperative. As mentioned earlier, the changes in the CD ellipticity measured by Kortemme et al. are also very nearly linear as a function of temperature, with only a slight toe at temperatures below 12 °C, which they interpreted as evidence of cooperative thermal unfolding. More importantly, we find no evidence for a stable β-sheet topology for Betanova even at the lowest temperature in our measurements; the β-sheet content is estimated to be less than 26% at 5 °C from both the CD and the FTIR analysis. The CD and FTIR measurements are not conclusive regarding the extent of disruption of the secondary structure content in Betanova with increasing temperatures, because they indicate a largely unstructured peptide at all temperatures. The primary conclusions we can draw are that although the secondary structure content of Betanova changes somewhat with increasing temperature, the changes are gradual and noncooperative.

The most novel finding of this study is from direct measurements of the changes in the FRET efficiency between donor and acceptor labels attached to the two ends. Our FRET measurements are consistent with the conclusion that Betanova has a largely unstructured conformation, even at low temperatures. In fact, the average end-to-end distance estimated from FRET, ~45 Å for Betanova at 25 °C, is more suggestive of that expected for a random coil for a polypeptide of that length than of a β-sheet structure. For a random coil, the end-to-end distance squared is given by the equation $\langle r^2 \rangle \approx C_n n l^2$, where n is the number of peptide bonds, l (~3.8 Å) is the distance between two successive C_α atoms along the length of the polypeptide, and C_n is the Flory constant and is approximately the ratio of the statistical segment length to the peptide bond length (*37*). Tanford et al. (*38*) estimated the end-to-end distance of a number of proteins in 6 M guanidine hydrochloride (with chain lengths varying from 26 to 1790 amino acids). From their measurements, we obtain a range of values for C_n from ~5.4 to ~7.6, with an average value for C_n of ~6.6. If we assume that our labeled peptide is approximately 23 residues long (we have attributed the extra length to the Lys at the C-terminus and the two fluorescent labels), we can estimate $\langle r^2 \rangle$ to be ~(46 Å)^2. This value is remarkably close to the average end-to-end distance estimated for Betanova from the FRET measurements.

There are several caveats to the calculations of the average end-to-end distance, both from FRET measurements and from random coil estimates. First, we have used a geometrical factor of $^2/_3$ in the calculation of the Forster distance R_o, which assumes that the emission and absorption dipoles of the donor and the acceptor molecules have random orientations relative to each other. The assumption that the

[2] The emission spectra of TMR-Betanova-FL show almost no TMR spectra, suggesting that the quantum yield of TMR attached to Betanova is very small. Direct excitation of TMR (at 543 nm) also shows that the fluorescence emission from TMR-Betanova-FL is a factor of ~10 smaller than that from TMR-^{D}P^{D}P-FL (data not shown).

fluorophores have random orientations is most likely not a bad approximation for labels attached to the ends of the peptides, especially since FL is attached to the amino group of Lys at the C-terminus. The geometric factor of $^2/_3$ is valid if even one of the fluorophores has complete reorientational freedom. Nevertheless, it is an assumption we have not experimentally verified. Second, we measure average FRET efficiencies, from which we can obtain the average end-to-end distances only if we know the distribution of conformations adopted by the peptide under each set of conditions. Our data show that the conformation of Betanova is primarily unstructured, but it is not straightforward to guess, a priori, what the distribution of conformations may be. Therefore, our estimate of average distances is only approximate. Third, the Flory constant C_n depends on the sequence of the polypeptide (*39*−*41*), and moreover, these peptides are not long enough for the Gaussian chain limit to be strictly valid. Nonetheless, the remarkable agreement between the experimentally obtained and theoretical values of the end-to-end distance provides confidence that our FRET measurements give reasonable estimates of the end-to-end distances in Betanova, and corroborates our conclusions from the CD and FTIR analysis that the conformation of Betanova is not very structured.

Our conclusions from FRET measurements on Betanova are also in agreement with results from FRET between Y10 and W3, monitored using fluorescence changes in Y10. These measurements showed that the fluorescence of Y10 is a factor of ∼2 smaller than the corresponding fluorescence in a reference peptide GKYTN. If we assume that the decrease in the fluorescence of Y10 relative to that of GKYTN is solely from resonance energy transfer between Y10 and W3, we can estimate that the distance between Y10 and W3 is approximately the Forster distance for Tyr and Trp in Betanova. Under denaturing conditions, we can make the assumption that Y10 and W3 have random orientation relative to one another, which gives a Forster distance of ∼14 Å between Tyr and Trp (*27*), and therefore ∼14 Å as the distance between Y10 and W3 at 80 °C or at 9.75 M urea. This estimate is in good agreement with the distance of ∼14 Å between the centers of Y10 and W3 observed in molecular dynamics simulations of Betanova for transiently more open conformations (J. Hilario and T. A. Keiderling, unpublished results). At low temperatures and with no denaturant, the distance between Y10 and W3 is estimated to be ∼12 Å from the FRET analysis, which is significantly larger than the distance of ∼8 Å obtained from the NMR coordinates (Figure 7). This analysis is, at best, qualitative, since it assumes a Forster distance of 14 Å under all conditions.

Bursulaya and Brooks (*2*, *23*) have done an extensive study on the conformational stability of Betanova using molecular dynamics (MD) simulations; they have calculated the free energy surface of Betanova at 2 °C along various coordinates such as the radius of gyration, the fraction of native tertiary contacts, and the number of hydrogen bonds. Their calculations suggest a two-stage collapse mechanism for Betanova at ∼2 °C. In the first stage, the unfolded conformations collapse into a large basin of compact states with native contacts ranging from 10 to 60% and no significant hydrogen bond formation. In the second stage, the polypeptide adopts the native β-sheet topology with ∼70% native contacts and 43−100% hydrogen bonds formed. What is most notable from their simulations is that the potential of mean force versus the fraction of native contacts is found to be essentially downhill with no significant barriers separating the native basin from the basin of collapsed states at low temperatures.

Both experiments and simulations suggest that Betanova is only marginally stable even at low temperatures, although there is a very wide variation in the estimates of β-sheet population in Betanova. In particular, our CD and FTIR measurements indicate a very low (≤26%) β-sheet population at 5 °C, which is considerably less than the estimate of 80−90% β-sheet at 5 °C by Serrano and co-workers from their original NMR and CD measurements (*19*). Boyden and Asher have estimated ∼63% β-sheet population from their UVRR studies (*21*) based on a fit to basis spectra empirically derived for α-helix, β-sheet, and disordered structures from the UVRR spectra of 13 proteins with well-known X-ray crystal structures (*42*). Furthermore, they conclude that the peptide retains β-sheet structure even at 80 °C based on their observation that their UVRR spectra do not change significantly between 5 and 82 °C when excited at 206.5 nm, which excites the peptide bond transition. They do observe a loosening of the hydrophobic core as monitored by changes in the UVRR spectra when excited at 229 nm, which excites the aromatic side chain transitions. One explanation, consistent with our results, for why Boyden and Asher do not see any changes in their peptide UVRR spectra is that Betanova is largely unstructured even at 5 °C, and that their result of ∼63% β-sheet population at all temperatures is an overestimate. As acknowledged by Boyden and Asher, it is difficult to make accurate estimates of β-sheet content from their UVRR spectra. The reference spectra they use for random coil and β-sheet differ primarily in amplitude, with very little shape changes, and moreover, the reference spectra differ quite significantly from the measured peptide spectrum. They assume, erroneously, a mostly folded peptide at 5 °C based on the original work of Serrano and co-workers (*19*) and on the results of the MD simulation (*2*), both of which had indicated a stability of ∼0.6−1 kcal/mol between 2 and 5 °C. More recently, Serrano and co-workers have re-estimated the β-sheet population in Betanova and report only ∼10% β-sheet in aqueous solution (*22*), significantly less than what they had reported in their original study, and much more in agreement with our results.

The measurements reported in this paper indicate an ensemble of structures even under "native-like" conditions, and provide new insight into the extent to which these model peptides are actually "folded" into the conformation described by the NMR parameters. The FRET measurements, together with the CD and FTIR measurements, show that the conformation of Betanova is largely that of an unstructured peptide, with no cooperative unfolding under thermal or chemical denaturation. The absence of a cooperative transition in our experimental studies corroborates the finding of the MD simulation studies that there is no significant barrier between the folded and unfolded conformations. The lack of cooperativity in all the unfolding transitions that were measured, with perhaps the exception of changes in Y10 fluorescence, suggests that there is a nearly continuous ensemble of secondary structure states, with a small fraction of peptides whose compact topology is stabilized by interstrand hydrogen bond formation as shown by the NMR

results of Kortemme et al. (*19*). It appears that the strength of the hydrophobic interactions in Betanova is not sufficient to compensate for the loss of conformational entropy.

The second peptide in this study, $^{D}P^{D}P$, exhibits more typical β-sheet-like CD and FTIR spectra at low temperatures, and its thermal denaturation shows a much larger change in these spectra than in the spectra of Betanova. However, as for Betanova, the CD and FTIR spectra do not exhibit any cooperativity in the thermal unfolding of $^{D}P^{D}P$. The average end-to-end distances between the fluorescent probes attached to $^{D}P^{D}P$, obtained from the FRET measurements, are in remarkable agreement with the distance estimated for probes attached to the ends of a three-stranded β-sheet topology, thus confirming the stable β-sheet-like topology for $^{D}P^{D}P$. The surprising result here is that, although the CD and FTIR spectral changes from ∼8 to ∼80 °C indicate that the peptide loses a significant amount of its secondary structure, the FRET efficiency does not change very much with temperature. Even with increased urea concentrations, this peptide remains in a collapsed state with little change in FRET efficiency. This may well be a consequence of the strong propensity of D-Pro-Gly sequences to form highly stable turns persisting even under denaturing conditions. We have been able to obtain consistent CD and FTIR spectra for these D-Pro-Gly sequences for model systems as short as a tetrapeptide (J. Hilario, J. Kubelka, and T. A. Keiderling, manuscript submitted to *J. Am. Chem. Soc.*).

Our primary conclusion from the thermodynamic stability measurements on short designed β-sheet-forming peptides is that the interstrand hydrogen bonds that stabilize β-sheets are formed noncooperatively. The lack of cooperativity in the thermal denaturation of both peptides raises the question of how cooperative small β-sheet-forming peptides are. The one system for which cooperative folding and unfolding are well-documented is the β-hairpin from protein GB1, which appears to be a "two-state" folder by several indicators. In response to a laser temperature jump (T-jump), this hairpin exhibits identical single-exponential kinetics when monitored by the change in the fluorescence of a single Trp that is partly buried in a hydrophobic cluster and by energy transfer from Trp to a dansylated Lys at the C-terminus (*15*). Furthermore, the equilibrium unfolding of this hairpin, monitored by NMR, shows that the temperature dependencies of the chemical shifts of all C_α protons except that at one end of the peptide overlap (*14*). A caveat that is worth noting is that the CD spectrum of this peptide does not show a typical β-sheet spectrum (*43*), a puzzling fact that remains to be explained. Moreover, the folding−unfolding transition as monitored by CD at 201 nm (*43*) appears to be much broader than the transition monitored by Trp fluorescence (*15*). Despite the unusual CD spectrum, the data strongly argue that this peptide exhibits a two-state folding−unfolding transition.

The evidence for cooperative folding and unfolding is not so straightforward for β-sheet-forming peptides. The most extensively studied β-sheet structure is the three-stranded β-sheet of the WW domain. Here the experimental data are more complex. The kinetics of folding and unfolding, initiated by a laser T-jump and monitored using Trp fluorescence (*18*), are single-exponential, as in the case of the β-hairpin. The equilibrium thermal and denaturant unfolding of WW, however, shows deviations expected for a simple two-state system (*17*). The temperature-dependent change in the ellipticity at 230 nm, which originates from the contribution of aromatic amino acids to the far-UV CD spectrum, the ellipticity measurements in the near-UV CD (at 290 nm), and Trp fluorescence changes, all of which probe the disruption of the hydrophobic cluster formation, exhibit sigmoidal transitions (*17*). It is not straightforward to compare the disruption of the hydrophobic cluster with the loss of secondary structure for this peptide because the CD spectrum of WW in the far-UV is not that of a typical β-sheet, presumably because of the contributions from the disordered tails at the N- and C-termini (*17*), and the change in ellipticity in the far-UV region (195−215 nm) is very small. With increasing urea concentrations, the WW domain exhibits a cooperative transition when monitored by Trp fluorescence, but a noncooperative change in ellipticity at 290 nm. Furthermore, the near-UV CD spectrum, which monitors the aromatic side chains, shows a significant signal from hydrophobic clustering even at 6 M urea or 5 M guanidine hydrochloride (*17*). Even for the WW domain, which is an example of the most cooperative β-sheet system, the β-sheet-like structure, as monitored by both CD and FTIR, disappears when the tails are removed as does any indication of cooperative unfolding, monitored by CD and Trp fluorescence; these results strongly suggest that tertiary interactions of the β-sheet with the tails are responsible for the stable secondary structure (*44*).

Recently, Cochran et al. have demonstrated that the tryptophan zipper peptide (trpzip) adopts a β-hairpin conformation that is stabilized by the formation of Trp-Trp hydrophobic clusters (*45*). The CD spectrum of trpzip has intense exciton-coupled bands at 215 and 229 nm (*45*). The distinctly sigmoidal changes observed in the CD spectra at 229 nm with increasing temperatures thus reflect the disruption of the hydrophobic cluster, and not changes in the extended secondary structure as monitored by far-UV CD or FTIR. Cochran et al. conclude from these measurements that the peptide unfolds cooperatively. However, preliminary FTIR data on the trpzip analogue with an NG-based turn show thermal unfolding that involves an intermediate state when one specifically investigates the secondary structure with a spectroscopic probe (V. Setnicka, J. Hilario, and T. A. Keiderling, unpublished results). Further studies are therefore necessary to establish cooperativity in this peptide.

It is very likely that cooperativity in β-sheet proteins arises from tertiary contacts that are lacking in small peptides and that a broad transition is more the norm than the exception here. In fact, even for helices that fold in isolation, independent of tertiary contacts, NMR and vibrational spectroscopy measurements show deviations from strict two-state behavior (*4*, *46*). In particular, experiments employing isotope labeling show that the peptides unfold via a series of intermediate structures (*4*). MD simulation studies of helix formation kinetics for an Ala pentapeptide showed that the kinetics can be described as downhill diffusion on a broad energy landscape without a significant free energy barrier separating the helical and unstructured conformations (*3*). The authors of this study predict nonexponential kinetics for helix formation and, more interestingly, relaxation kinetics that depend on the initial distribution of the unstructured conformations and hence the initial temperature of the T-jump. Recent experiments on an Ala-based helical peptide,

using infrared spectroscopy to probe changes in conformations after a laser T-jump, confirm nonexponential kinetics that do indeed depend on the initial and final temperatures (*5*).

It is clear that a more complete picture of the underlying free energy landscape of β-sheets will come from extending the thermodynamics measurements reported in this study to kinetics measurements. In particular, to pursue the relative importance of hydrophobic cluster formation versus interstrand hydrogen bonding, it will be necessary to compare the kinetics obtained from Trp fluorescence and FRET measurements with a direct probe of the kinetics of secondary structure formation as from time-resolved infrared measurements (*5*, *47*, *48*).

ACKNOWLEDGMENT

We are very grateful to Samuel H. Gellman for providing us with a sample of the cyclic peptide so that we could obtain a reference CD spectrum and to Tanja Kortemme for providing us with the NMR coordinates of Betanova.

REFERENCES

1. Gellman, S. H. (1998) *Curr. Opin. Chem. Biol. 2*, 717−725.
2. Bursulaya, B. D., and Brooks, C. L., III (1999) *J. Am. Chem. Soc. 121*, 9947−9951.
3. Hummer, G., Garcia, A. E., and Garde, S. (2000) *Phys. Rev. Lett. 85*, 2637−2640.
4. Silva, R. A., Kubelka, J., Bour, P., Decatur, S. M., and Keiderling, T. A. (2000) *Proc. Natl. Acad. Sci. U.S.A. 97*, 8318−8323.
5. Huang, C. Y., Getahun, Z., Zhu, Y., Klemke, J. W., DeGrado, W. F., and Gai, F. (2002) *Proc. Natl. Acad. Sci. U.S.A. 99*, 2788−2793.
6. Blanco, F. J., Rivas, G., and Serrano, L. (1994) *Nat. Struct. Biol. 1*, 584−590.
7. Searle, M. S., Williams, D. H., and Rackman, L. C. (1995) *Nat. Struct. Biol. 2*, 999−1006.
8. Blanco, F., Ramirez-Alvarado, M., and Serrano, L. (1998) *Curr. Opin. Struct. Biol. 8*, 107−111.
9. Schenck, H. L., and Gellman, S. H. (1998) *J. Am. Chem. Soc. 120*, 4869−4870.
10. Sharman, G. J., and Searle, M. S. (1998) *J. Am. Chem. Soc. 120*, 5291−5300.
11. de Alba, E., Santoro, J., Rico, M., and Jimenez, M. A. (1999) *Protein Sci. 8*, 854−865.
12. Booth, D. R., Sunde, M., Bellotti, V., Robinson, C. V., Hutchinson, W. L., Fraser, P. E., Hawkins, P. N., Dobson, C. M., Radford, S. E., Blake, C. C., and Pepys, M. B. (1997) *Nature 385*, 787−793.
13. Kelly, J. W. (1997) *Structure 5*, 595−600.
14. Honda, S., Kobayashi, N., and Munekata, E. (2000) *J. Mol. Biol. 295*, 269−278.
15. Munoz, V., Thompson, P. A., Hofrichter, J., and Eaton, W. A. (1997) *Nature 390*, 196−199.
16. Munoz, V., Henry, E. R., Hofrichter, J., and Eaton, W. A. (1998) *Proc. Natl. Acad. Sci. U.S.A. 95*, 5872−5879.
17. Koepf, E. K., Petrassi, H. M., Sudol, M., and Kelly, J. W. (1999) *Protein Sci. 8*, 841−853.
18. Crane, J. C., Koepf, E. K., Kelly, J. W., and Gruebele, M. (2000) *J. Mol. Biol. 298*, 283−292.
19. Kortemme, T., Ramirez-Alvarado, M., and Serrano, L. (1998) *Science 281*, 253−256.
20. Hilario, J., and Keiderling, T. A. (2001) *Biophys. J. 80*, 557a.
21. Boyden, M. N., and Asher, S. A. (2001) *Biochemistry 40*, 13723−13727.
22. Lopez de la Paz, M., Lacroix, M., Ramirez-Alvarado, M., and Serrano, L. (2001) *J. Mol. Biol. 312*, 229−246.
23. Bursulaya, B. D., and Brooks, C. L., III (2000) *J. Phys. Chem. B 104*, 12378−12383.
24. Haas, E., Wilchek, M., Katchalski-Katzir, E., and Steinberg, I. Z. (1975) *Proc. Natl. Acad. Sci. U.S.A. 72*, 1807−1811.
25. Beechem, J. M., and Haas, E. (1989) *Biophys. J. 55*, 1225−1236.
26. Buckler, D. R., Haas, E., and Scheraga, H. A. (1995) *Biochemistry 34*, 15965−15978.
27. Lakowicz, J. R. (1983) *Principles of fluorescence spectroscopy*, Plenum Press, New York.
28. Shen, J., and Snook, R. D. (1989) *Chem. Phys. Lett. 155*, 583−586.
29. Henry, E. R., and Hofrichter, J. (1992) *Methods Enzymol. 210*, 129−192.
30. Cantor, C. R., and Timasheff, S. N. (1982) in *The proteins* (Neurath, H., and Hill, R. L., Eds.) Academic Press, New York.
31. Syud, F. A., Espinosa, J. F., and Gellman, S. H. (1999) *J. Am. Chem. Soc. 121*, 11577−11578.
32. Manning, M. C., and Woody, R. W. (1987) *Biopolymers 26*, 1731−1752.
33. Sreerama, N., and Woody, R. W. (2000) in *Circular Dichroism: Principles and Applications* (Berova, N., and Woody, R. W., Eds.) 2nd ed., pp 601−620, Wiley-VCH, New York.
34. Pancoska, P., Bitto, E., Janota, V., Urbanova, M., Gupta, V. P., and Keiderling, T. A. (1995) *Protein Sci. 4*, 1384−1401.
35. Byler, D. M., and Susi, H. (1986) *Biopolymers 25*, 469−487.
36. Baumruk, V., Pancoska, P., and Keiderling, T. A. (1996) *J. Mol. Biol. 259*, 774−791.
37. Flory, P. J. (1969) *Statistical Mechanics of Chain Molecules*, Interscience Publishers, New York.
38. Tanford, C., Kawahara, K., and Lapanje, S. (1966) *J. Biol. Chem. 241*, 1921−1923.
39. Miller, W. G., Brant, D. A., and Flory, P. J. (1967) *J. Mol. Biol. 23*, 67−80.
40. Bieri, O., Wirz, J., Hellrung, B., Schutkowski, M., Drewello, M., and Kiefhaber, T. (1999) *Proc. Natl. Acad. Sci. U.S.A. 96*, 9597−9601.
41. Lapidus, L. J., Eaton, W. A., and Hofrichter, J. (2000) *Proc. Natl. Acad. Sci. U.S.A. 97*, 7220−7225.
42. Chi, Z., Chen, X. G., Holtz, J. S. W., and Asher, S. A. (1998) *Biochemistry 37*, 2854−2864.
43. Jas, G. S., Eaton, W. A., and Hofrichter, J. (2001) *J. Phys. Chem. B 105*, 261−272.
44. Hilario, J., and Keiderling, T. A. (2003) *Biophys. J. 84*, 161a.
45. Cochran, A. G., Skelton, N. J., and Starovasnik, M. A. (2001) *Proc. Natl. Acad. Sci. U.S.A. 98*, 5578−5583.
46. Rohl, C. A., and Baldwin, R. L. (1994) *Biochemistry 33*, 7760−7767.
47. Callender, R. H., Dyer, R. B., Gilmanshin, R., and Woodruff, W. H. (1998) *Annu. Rev. Phys. Chem. 49*, 173−202.
48. Dyer, R. B., Gai, F., Woodruff, W. H., Gilmanshin, R., and Callender, R. H. (1998) *Acc. Chem. Res. 31*, 709−716.

BI026893K